Available online at www.sciencedirect.com
ScienceDirect
International Journal of Mass Spectrometry 262 (2007) 136–143
International Journal of Mass Spectrometry
www.elsevier.com/locate/ijms

Parity alternation of linear ground-state C_nS^{2-} ($n = 6$–18) clusters

M.D. Chen [a,*], J. Liu [a], Q.B. Chen [a], Q.E. Zhang [a], C.T. Au [b]

[a] *State Key Laboratory of Physical Chemistry of Solid Surfaces, Department of Chemistry, College of Chemistry and Chemical Engineering, Center for Theoretical Chemistry, Xiamen University, Xiamen 361005, People's Republic of China*
[b] *Department of Chemistry, Hong Kong Baptist University, Kowloon Tong, Hong Kong, China*

Received 29 September 2006; received in revised form 6 November 2006; accepted 6 November 2006
Available online 6 February 2007

Abstract

Making use of the software of molecular graphics, we designed many patterns of C_nS^{2-} ($n = 6$–18) models. We carried out geometry optimization and calculation on vibrational frequency by means of the B3LYP density functional method. The most probable ground-state isomers of C_nS^{2-} ($n = 6$–18) are linear with the sulfur atom located at one end of the C_n chain. When n is even, the isomer is polyacetylene-like. The C_nS^{2-} ($n = 6$–18) with even number of carbon atoms are more stable than those with odd number, matching the peak pattern observed in studies of mass spectrometry. The trend of odd/even alternation is also detected in certain bond length, atomic charge, electronic configuration, the highest vibrational frequency, energy difference, electron detachment energy, and incremental binding energy of the most probable ground-state isomers.

Keywords: Binary cluster; Dianions; C_nS^{2-}; Sulfur-doped clusters; Density functional study

1. Introduction

During the last decade, much research has been directed towards the understanding of the structures and properties of small carbon clusters [1]. There are theoretical and experimental evidence that the formation of fullerenes and their isomers proceeds by a mechanism in which small carbon clusters undergo condensation from linear chains to monocyclic rings and finally to large three-dimensional structures [2]. Besides the C_n clusters, carbon clusters doped with a heteroatom have attracted immense attention. Besides their importance in relation to the reactivity of carbon clusters with heteroatom-doped molecules, these clusters are interesting because of the change in the properties of the carbon clusters caused by the presence of heteroatoms. Carbon chains doped with heteroatoms are also important in astrophysics. A variety of carbon clusters bonded to heteroatoms such as O, N, and S were observed in interstellar clouds; the small polycarbon sulfides C_nS ($n = 1$–3, 5) species have been observed in the envelopes of some interstellar clouds [3–5]. By means of laser ionization, a series of hetero-carbon anionic C_nX^- clusters were generated by adding a heteroatom X into the corresponding C_n^- clusters, where X is either a main group, a transition, or a non-metal element [6–10].

To explore the intriguing experimental observations, theoretical investigations on polycarbon sulfides were conducted. Zaidi et al. calculated the most stable linear isomer of C_3S in potential energy surface by CCSD(T) method [11]. Wang et al. calculated infrared spectra and dissociation pathways of linear C_nS_m ($n = 1$–29, $m = 1$–2) clusters and vibrational absorption spectra of C_nS ($n = 2, 6$) and C_nS_2 ($n = 7, 9, 11, 13, 15$) linear carbon–sulfur clusters using B3LYP/6-311G* DFT methods [12,13]. Pérez-Juste et al. examined linear sulfur–carbon chains C_nS ($n = 1$–6) of astronomical interest by means of several theoretical methods [14]. Tang and BelBruno investigated the structures and energies of C_nS^+ ($1 \leq n \leq 16$) and C_nS^- ($9 \leq n \leq 16$) by density functional method [15]. Lee and co-workers examined structures and spectroscopic properties of linear polycarbon sulfides C_nS ($n = 2$–9) and SC_nS ($n = 2$–6) by density functional theory calculations [16,17]. Pascoli and Lavendy studied structures and energies of C_nS ($1 \leq n \leq 20$) and C_nS^+ ($n = 1$–23) sulfur carbide clusters [18,19]. Flores et al. carried out a theoretical study of the excited electronic states of the SC_3 system by means of B3LYP, QCI, MRCI, and RHF-CC methods [20].

Compared to neutral and singly charged anionic and cationic hetero-carbon clusters, the doubly charged dianions behave very differently. Because of the strong Coulomb repulsion induced

---

[*] Corresponding author. Tel.: +86 592 2182332; fax: +86 592 2184708.
E-mail address: mdchen@xmu.edu.cn (M.D. Chen).

1387-3806/$ – see front matter © 2006 Elsevier B.V. All rights reserved.
doi:10.1016/j.ijms.2006.11.005

by the added electrons, small dianions are unlikely to exist as stable gas-phase entities [21]. There are only a small number of experimental and theoretical investigations on hetero-carbon dianion clusters. Schauer et al. observed stable carbon dianions C_n^{2-} ($7 \leq n \leq 28$) [22]. Klein and Middleton observed BeC_n^{2-} ($n=4$–14) by accelerator mass spectrometry and Coulomb Explosion Imaging [23]. Gnaser et al. produced SiC_n^{2-} ($n=6$, 8, 10) and OC_n^{2-} ($n=5$–19) in sputtering [24,25]. Franzreb and Williams reported the observation of novel classes of mixed dianions SC_n^{2-} ($6 \leq n \leq 18$), $O_2C_7^{2-}$, $C_nH_m^{2-}$ ($n \geq 7$), $BeC_8H_m^{2-}$, $SiOC_n^{2-}$ ($n=4$, 6, 8), and $SiO_2C_n^{2-}$ ($n=4$, 6) by sputtering and gas flooding [26]. Dreuw et al. carried out theoretical studies on $Si_xC_y^{2-}$ ($x=1$, 2, $y=4$–9) [27,28], OC_n^{2-} ($n=5$–8) [25], and BeC_n^{2-} ($n=4$, 6) [29] by means of standard *ab initio* methods. Shi and Kais conducted *ab initio* calculation of the repulsive Coulomb barrier for several geometrically stable isomers of C_4Be^{2-} dianions [30]. Trindle and Yumak developed a set of small open shell stable dianions by means of ROMP2, CCSD and DFT calculations [31]. Earlier, we carried out a B3LYP density functional study on beryllium-doped carbon dianion C_nBe^{2-} ($n=4$–14) clusters [32].

In the dianion abundance patterns of SC_n^{2-} ($6 \leq n \leq 18$) anions for SF_6 flooding of graphite [26], the dianionic clusters show an obvious odd/even behavior: the dianions with even number of carbon atoms are more prominent. To explore the experimental observation theoretically, we designed many structural models of C_nS^{2-} ($n=6$–18), and performed geometry optimization and calculations on vibrational frequencies by means of the B3LYP density functional method. The geometry structure, bonding character, atomic charge, electronic configuration, the highest vibrational frequency, energy difference, electron detachment energy, and incremental binding energy of the most probable ground-state (denoted as "ground-state" hereinafter) dianionic clusters were examined. Based on the results, we provide explanation on why the C_nS^{2-} ($n=6$–18) isomers with even *n* are more stable than those with odd *n*. The outcome can serve as a guideline for the synthesis of related materials as well as for future theoretical studies of carbon/sulfur binary clusters.

2. Computational methods

During the investigation, devices for molecular graphics, molecular mechanics, and quantum chemistry were used. First, a three-dimensional model of a cluster was designed using HyperChem for Windows [33] and Desktop Molecular Modeller [34] on a PC/Pentium IV computer. Then, the model was optimized by MM+ molecular mechanics and semi-empirical PM3 quantum chemistry. Last, geometry optimization and calculations of vibrational frequencies were conducted using the B3LYP density functional method of Gaussian 03 package [35] with 6-311G* basis sets, i.e., Becke's three-parameter non-local exchange functional with the correlation functional of Lee–Yang–Parr [36,37]. It has been pointed out that geometries computed with more expensive basis sets do not necessarily lead to more accurate final results [38]. The single point energy calculations following the optimizations were performed using the larger 6-311+G* basis set (i.e., B3LYP/6-311+G*//B3LYP/6-311G*). Since the change of zero point energy (ZPE) could only be affected slightly by the quality of the employed method [29], all energies were calculated with ZPE correction at the B3LYP/6-311G* level. The optimized models were again displayed using HyperChem for Windows. The data of partial charges and bond orders were explored with Gaussian Natural Bond Orbital (NBO). All of the calculations were carried out on the servers of SGI.

Though DFT is a method based on one-determinant approximation, its use on dianions is still in dispute. Trindle and Yumak developed a set of small open shell dianions stable, their results of B3LYP/6-31+G(d) description of the carbene-based systems are in impressive agreement with ROMP and CCSD calculations on the same basis, and they considered that the calculations in a modest basis and in the B3LYP variant of DFT are trustworthy [31]. In the study on C_nBe^{2-} ($n=4$–14), we also performed B3LYP/6-311+G* calculations on the structures and energies of the clusters [32]. In the present studies, we examined many isomers and made comparison for the identification of the "ground-state" isomers, and focused on the common trends of odd/even parity alternation. Considering the fact that B3LYP requires significantly less computing efforts than the other methods of similar accuracy that include electron correlation, the present method can be employed for treating the medium-sized clusters efficiently in an economical and affordable manner.

3. Results and discussion

3.1. Geometry configuration

At the beginning of the study, nothing was known other than the C_nS^{2-} ($n=6$–18) formula. The assumption of a reasonable geometrical structure was the initial step for the optimization of the new dianions. First, we examined a large number of possible models which are reasonable in chemical understandings, among which are linear, cyclic, and bicyclic, as well as three-dimensional structures. After a number of trial optimizations, the results are summarized and models with imaginary vibrational frequencies and/or of higher energies are discarded. Nine main categories of C_nS^{2-} ($n=6$–18) structures are summarized and displayed in Fig. 1. Category 1a denotes the "ground-state" isomers with linear structures. Categories 1b and 1c are bent chain structures with a sulfur atom located at or around the middle of the chain, and the corresponding linear configurations have imaginary frequencies. Category 1d is "Y" shape in structure with the sulfur atom located at the end of one of the three carbon branches. Category 1e is also a sort of "Y" structure with one of the three branches being a C–S bond. Category 1f is a carbon ring connected to a C_xS chain with the sulfur atom located at the end of the chain. Category 1g is a structure with the sulfur atom of a carbon–sulfur ring connected to a carbon chain. Category 1h is a carbon ring containing a sulfur atom. Category 1i is with a sulfur atom connected to one of the carbon atoms of a carbon ring.

Because of the fact that there are numerous isomers in the structures of the clusters, the identification of the ground state is important. For a particular family of molecules, the basic struc-

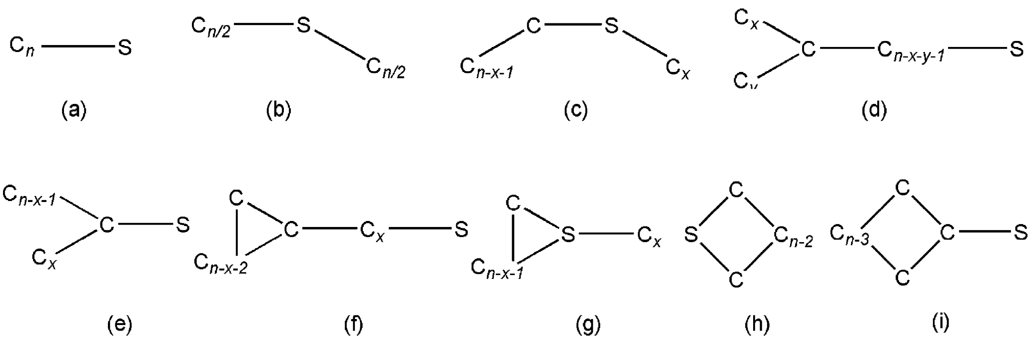

Fig. 1. Nine main categories of C_nS^{2-} ($n=6$–18) structures (x and y denote the number of carbon atom(s), respectively).

ture with the lowest energy affects the "building up" of larger molecules, and this is an important area in biochemical research. In previous theoretical investigations on C_nS, C_nS^+, and C_nS^- clusters, a configuration with the sulfur atom located at the terminus of a linear carbon chain is probably the most favorable in energy [12–16,18,19]. The most stable structures of C_nS_2 are also suggested to be linear with one sulfur atom located at each end of the carbon chain [12,13,17]. After comparing a great number of models, we find that the "ground-state" isomers of C_nS^{2-} ($n=6$–18) clusters are linear in configuration having a sulfur atom at a terminal position. For the beryllium-doped carbon dianion clusters C_nBe^{2-} ($n=4$–14), the linear configuration with the beryllium atom located at the end of a carbon chain is not the most stable isomers; those found with the lowest energy are having the beryllium atom located inside the carbon chain [32].

3.2. Bond characters

Depicted in Table 1 are the bond lengths for the "ground-state" C_nS^{2-} ($n=6$–18) clusters. According to the results of calculation, the lengths of C–S are within the 1.626–1.684 Å range, exhibiting essentially the characteristic of single bond. The bond lengths of the last C–C bonds at the terminus of the chain are within 1.255–1.275 Å, and there is a trend of odd/even alternation: for even n, the lengths are within 1.256–1.262 Å; for odd n, the lengths are within 1.266–1.275 Å. Shown in Fig. 2 are bond lengths of the last C–C bond of the "ground-state" C_nS^{2-} ($n=6$–18) clusters versus the number of carbon atoms. The bonding of small linear carbon chains could be cumulene- or polyacetylene-like [39]. Along the straight carbon chains of the "ground-state" C_nS^{2-} ($n=6$–18) isomers, there is an alternate short/long pattern in C–C bond lengths when n is even, and the C–C bonds display a typical polyacetylene-like character, i.e., appearing as a series of alternate single and triple bonds. When n is odd, there is also a sort of short/long alternation of the C–C bond lengths but such feature fades out gradually from both terminuses towards the center of the chain, and the C–C bond lengths near the chain center tend to average out, exhibiting some sort of cumulenic character (with two double bonds). As an illustration, depicted in Fig. 3 are the bond lengths of the "ground-state" $C_{17}S^{2-}$ and $C_{18}S^{2-}$ clusters versus the number of bond (as counted from the top in Table 1, e.g., the C–S bond length is plotted against "1" and so on), the curve

Table 1
Bond lengths (in Å) for the "ground-state" C_nS^{2-} ($n=6$–18) clusters (R_{SC} is the S–C bond length and the subscript numbers of "R" refer to bonds counting from the side of S–C bond)

	C_6S^{2-}	C_7S^{2-}	C_8S^{2-}	C_9S^{2-}	$C_{10}S^{2-}$	$C_{11}S^{2-}$	$C_{12}S^{2-}$	$C_{13}S^{2-}$	$C_{14}S^{2-}$	$C_{15}S^{2-}$	$C_{16}S^{2-}$	$C_{17}S^{2-}$	$C_{18}S^{2-}$
R_{SC}	1.685	1.668	1.666	1.655	1.654	1.646	1.644	1.638	1.636	1.631	1.631	1.627	1.626
R_1	1.234	1.254	1.237	1.251	1.240	1.250	1.242	1.250	1.244	1.250	1.246	1.250	1.247
R_2	1.359	1.320	1.348	1.322	1.340	1.322	1.334	1.320	1.329	1.318	1.325	1.317	1.321
R_3	1.236	1.288	1.237	1.273	1.239	1.264	1.241	1.260	1.243	1.258	1.244	1.256	1.246
R_4	1.365	1.282	1.348	1.294	1.341	1.302	1.335	1.306	1.331	1.307	1.327	1.309	1.324
R_5	1.255	1.331	1.238	1.301	1.239	1.285	1.240	1.275	1.241	1.269	1.242	1.264	1.244
R_6		1.275	1.355	1.267	1.341	1.280	1.336	1.288	1.333	1.293	1.329	1.298	1.327
R_7			1.256	1.333	1.239	1.307	1.240	1.293	1.240	1.284	1.241	1.276	1.242
R_8				1.270	1.348	1.260	1.336	1.270	1.333	1.277	1.330	1.284	1.329
R_9					1.259	1.332	1.240	1.311	1.241	1.300	1.241	1.290	1.241
R_{10}						1.268	1.343	1.256	1.332	1.263	1.330	1.271	1.329
R_{11}							1.259	1.331	1.242	1.313	1.241	1.303	1.241
R_{12}								1.267	1.338	1.253	1.329	1.260	1.328
R_{13}									1.260	1.330	1.243	1.314	1.242
R_{14}										1.266	1.335	1.252	1.326
R_{15}											1.261	1.329	1.244
R_{16}												1.266	1.333
R_{17}													1.262

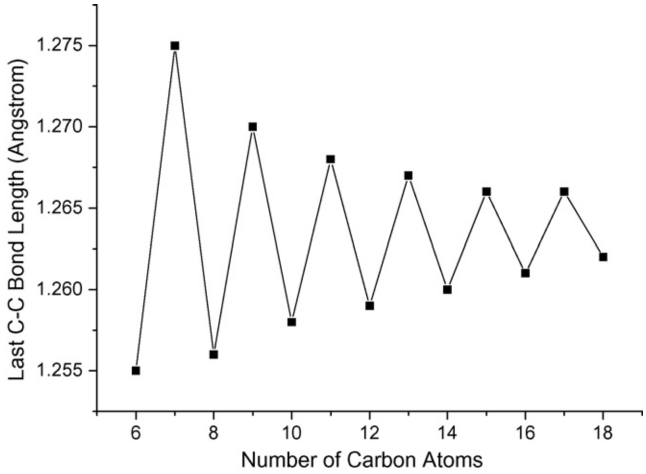

Fig. 2. Lengths of the last C—C bond (in Å) of the "ground-state" C_nS^{2-} ($n = 6$–18) clusters vs. the number of carbon atoms.

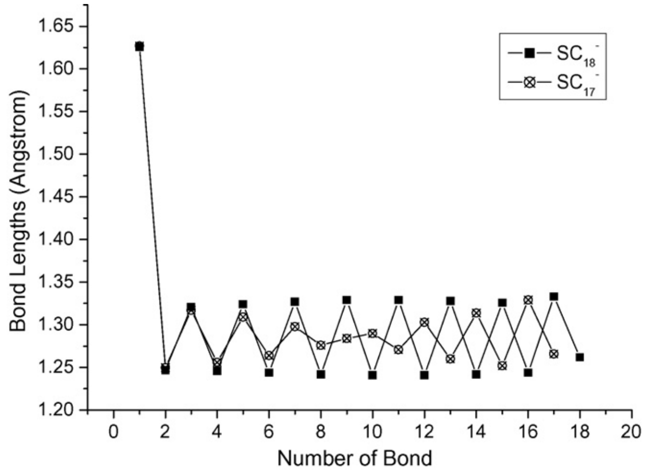

Fig. 3. Bond lengths (in Å) of the "ground-state" $C_{17}S^{2-}$ and $C_{18}S^{2-}$ clusters vs. the number of bond (as counted from the top in Table 1).

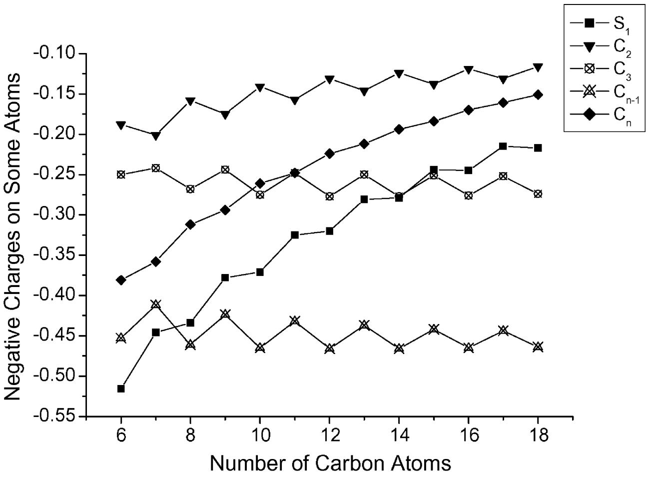

Fig. 4. Negative charge on some atoms of the "ground-state" C_nS^{2-} ($n = 6$–18) clusters vs. the number of carbon atoms.

of the $C_{18}S^{2-}$ with polyacetylene-like carbon chain displays classical short/long alternation, whereas that of $C_{17}S^{2-}$ exhibits polyacetylene-like at the two terminuses of the carbon chain and with some sign of cumulene-like near the center (i.e., averaging out). The results of NBO bond order analysis confirm the above bonding characters.

NBO atomic charges of the "ground-state" C_nS^{2-} ($n = 6$–18) clusters are listed in Table 2. Shown in Fig. 4 are negative charges on some atoms of the "ground-state" C_nS^{2-} ($n = 6$–18) clusters versus the number of carbon atoms. The sulfur atoms have negative charge (in the range of −0.217 to −0.516), the level of the negativity decreases with a rise in *n*, showing slight odd/even alternation in the extent of decrease in negative charging. On the carbon atom bonded to the sulfur atom, there is some sort of small/large alternation of negative charges with odd/even *n*: the negative charge at the carbon atom bonded to the sulfur atom of an even *n* structure is smaller than that of the neighboring odd-*n* isomers. The third carbon atoms counted from the sulfur

Table 2
NBO atomic charges of the "ground-state" C_nS^{2-} ($n = 6$–18) clusters

	C_6S^{2-}	C_7S^{2-}	C_8S^{2-}	C_9S^{2-}	$C_{10}S^{2-}$	$C_{11}S^{2-}$	$C_{12}S^{2-}$	$C_{13}S^{2-}$	$C_{14}S^{2-}$	$C_{15}S^{2-}$	$C_{16}S^{2-}$	$C_{17}S^{2-}$	$C_{18}S^{2-}$
S_1	−0.516	−0.446	−0.434	−0.378	−0.371	−0.325	−0.320	−0.281	−0.279	−0.244	−0.245	−0.215	−0.217
C_2	−0.188	−0.201	−0.158	−0.175	−0.141	−0.157	−0.131	−0.146	−0.124	−0.138	−0.119	−0.131	−0.116
C_3	−0.250	−0.242	−0.268	−0.244	−0.275	−0.248	−0.277	−0.250	−0.277	−0.251	−0.276	−0.252	−0.274
C_4	−0.143	−0.101	−0.067	−0.068	−0.022	−0.038	0.007	−0.014	0.027	0.005	0.041	0.020	0.051
C_5	−0.068	−0.162	−0.118	−0.137	−0.142	−0.131	−0.155	−0.132	−0.162	−0.134	−0.010	−0.137	−0.167
C_6	−0.453	−0.075	−0.170	−0.094	−0.100	−0.084	−0.057	−0.066	−0.029	−0.049	−0.018	−0.033	0.005
C_7	−0.381	−0.412	−0.012	−0.152	−0.065	−0.113	−0.092	−0.100	−0.107	−0.096	−0.116	−0.096	−0.122
C_8		−0.358	−0.461	−0.033	−0.181	−0.073	−0.115	−0.077	−0.074	−0.069	−0.047	−0.058	−0.027
C_9			−0.312	−0.424	−0.023	−0.155	−0.032	−0.106	−0.059	−0.086	−0.075	−0.078	−0.086
C_{10}				−0.294	−0.465	−0.000	−0.186	−0.050	−0.124	−0.064	−0.085	−0.064	−0.058
C_{11}					−0.261	−0.432	0.048	−0.155	−0.008	−0.106	−0.036	−0.081	−0.052
C_{12}						−0.248	−0.466	0.026	−0.189	−0.030	−0.130	−0.050	−0.093
C_{13}							−0.224	−0.437	0.066	−0.159	0.009	−0.107	−0.018
C_{14}								−0.212	−0.466	0.046	−0.190	−0.014	−0.133
C_{15}									−0.194	−0.442	0.079	−0.162	0.022
C_{16}										−0.184	−0.465	0.062	−0.190
C_{17}											−0.170	−0.444	0.090
C_{18}												−0.161	−0.464

terminus show an odd/even alternation “inverse” to that of the previous carbon atom with higher level of negative charging. From the other terminus, the last carbon atom has a negative charge in the range of −0.151 to −0.381, and the level of the negative charge decreases with a rise in n. The highest level of negative charge is on the second last carbon atom. There is also an odd/even trend of alternate charging: the negative charge of the second last carbon atom with n even is larger than that with n odd.

The strong force of Coulomb repulsion of a doubly charged anion would either enhance the emission of an electron or promote the decomposition of the molecular framework into two monoanionic fragments [21]. For the C_nBe^{2-} ($n = 4$–14) clusters, the dianionic structures with the beryllium atom located inside the carbon chain are more stable than those with the beryllium atom located at the end of the carbon chain, because the interior beryllium atom plays an important role of reducing Coulomb repulsion by separating the two negative charges [32]. According to the NBO atomic charges shown in Table 2, the majority of negative charge is located on the sulfur atom and the two carbon atoms at the other end of the carbon chain. The distribution of negative charge on the other carbon atoms of the chain shows lower level of charge values. The sulfur atom is larger in electronegativity than that of metal atoms, and the negative charge distributed at the two ends of the chain could obviously reduce the Coulomb repulsion force of the charges and stabilize the linear structures.

3.3. Electronic configuration and valence-bond structures

The electronic configurations of the “ground-state” C_nS^{2-} ($n = 6$–18) clusters are summarized as

$$(\text{core})1\sigma^2\ldots1\pi^4\ldots(n+2)\sigma^2\left(\frac{n+2}{2}\right)\pi^4,\quad n\text{ is even}$$

$$(\text{core})1\sigma^2\ldots1\pi^4\ldots(n+2)\sigma^2\left(\frac{n+3}{2}\right)\pi^2,\quad n\text{ is odd}$$

The dianionic C_nS^{2-} ($n = 6$–18) clusters possess $(4n + 8)$ valance electrons, among which are $2n + 4$ σ and π electrons, respectively. The outermost doubly degenerate π orbitals of linear C_nS^{2-} clusters with even n are fully occupied ($^1\Sigma^+$ electronic state); for odd n, they are half-filled ($^3\Sigma^-$ electronic state). The HOMO with fully filled π orbitals is energetically more stable than that with a half-filled electron shell. The $^1\Sigma^+$ (even n) and $^3\Sigma^-$ (odd n) alternations arise from the fact that all MOs with π-symmetry are doubly degenerate. The addition of an extra carbon atom in singlet state (even n) would result in having two more electrons included in the π-system, these electrons are accommodated in a π-orbital resulting in a triplet state (odd n).

The dominant valence-bond structures in each case can be defined, respectively, as follows:

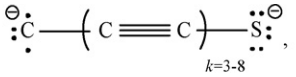

n is odd

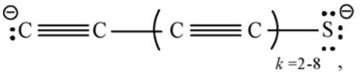

n is even

According to the above Lewis structure, the C–S bond exhibits a single bond. The last C–C bonds at the terminuses of the chains have odd/even alternation: triple bonds for even n, single bonds for odd n (as shown in Fig. 2). There is an alternate single/triple in C–C bond of the linear chain, displaying a polyacetylene-like character (as depicted in Fig. 3). The two negative charges located at the two terminuses of the chain could obviously reduce the Coulomb repulsion force and stabilize the linear structure. The sulfur is more electron-rich than the carbon atom, it helps to seal the terminal of the carbon chain, while beryllium is an electron-deficient element and is unlikely to be a terminal atom in the C_nBe^{2-} ($n = 4$–14) clusters [32]. When n is odd, the carbon atom at the end has two unpaired electrons and triplet structures are favorable. When n is even, due to the character of triple bonding at the end of chain, singlet is preferred.

3.4. Vibrational frequencies

According to the vibrational frequencies and intensities of the “ground-state” C_nS^{2-} ($n = 6$–18) clusters (supplementary data), there are n stretching modes that transform as the σ irreducible representation and $n - 1$ doubly degenerate bending modes; the latter transform as the π irreducible representation. It shows that the bending modes carry little intensity as expected. The intensities of the stretching modes are usually much larger than those of the bending modes. The highest frequency of the “ground-state” C_nS^{2-} ($n = 6$–18) clusters are 2192, 2012, 2194, 2056, 2206, 2097, 2221, 2117, 2230, 2144, 2230, 2156, and 2235 (cm^{-1}), respectively. Shown in Fig. 5 are the highest frequency of the “ground-state” C_nS^{2-} ($n = 6$–18) clusters versus the number of carbon atoms.

There is an odd/even pattern in the stretching mode of the highest frequency: the frequency of C_nS^{2-} is larger than $C_{n+1}S^{2-}$ for clusters with even numbers of carbon atoms and it is the other way round when n is odd. Similar feature was also noticed in C_nS ($n = 2$–9) and SC_nS ($n = 2$–6) clusters by Lee and co-workers [16,17]. It seems that the odd/even pattern observed

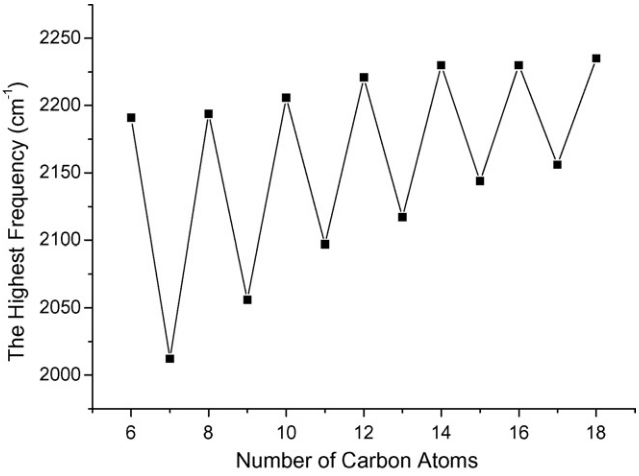

Fig. 5. The highest frequency (cm^{-1}) of the “ground-state” linear C_nS^{2-} ($n = 6$–18) clusters vs. the number of carbon atoms.

Table 3
Electronic states, total energies (a.u.), energy difference ΔE_n (a.u.), electron detachment energy EDE (a.u.), second electron detachment energy (SEDE) (a.u.), atomization energy ΔE_a (a.u.), and incremental binding energy ΔE^I (a.u.) of the "ground-state" C_nS^{2-} ($n = 6$–18) clusters

Cluster	State	Total energy	ΔE_n	EDE	SEDE	ΔE_a	ΔE^I
C_6S^{2-}	$^1\Sigma^+$	−626.7071		−0.0306	0.1599	1.4304	
C_7S^{2-}	$^3\Sigma^-$	−664.7768	−38.0697	−0.0481	0.1164	1.6429	0.2124
C_8S^{2-}	$^1\Sigma^+$	−702.9095	−38.1327	−0.0070	0.1631	1.9183	0.2754
C_9S^{2-}	$^3\Sigma^-$	−740.9807	−38.0712	−0.0220	0.1260	2.1322	0.2139
$C_{10}S^{2-}$	$^1\Sigma^+$	−779.1071	−38.1265	0.0137	0.1658	2.4014	0.2692
$C_{11}S^{2-}$	$^3\Sigma^-$	−817.1806	−38.0734	0.0009	0.1338	2.6175	0.2162
$C_{12}S^{2-}$	$^1\Sigma^+$	−855.2968	−38.1162	0.0290	0.1657	2.8765	0.2590
$C_{13}S^{2-}$	$^3\Sigma^-$	−893.3714	−38.0746	0.0177	0.1370	3.0939	0.2174
$C_{14}S^{2-}$	$^1\Sigma^+$	−931.4843	−38.1129	0.0426	0.1667	3.3495	0.2556
$C_{15}S^{2-}$	$^3\Sigma^-$	−969.5603	−38.0759	0.0328	0.1406	3.5682	0.2187
$C_{16}S^{2-}$	$^1\Sigma^+$	−1007.6670	−38.1072	0.0528	0.1663	3.8181	0.2499
$C_{17}S^{2-}$	$^3\Sigma^-$	−1045.7440	−38.0768	0.0441	0.1424	4.0377	0.2196
$C_{18}S^{2-}$	$^1\Sigma^+$	−1083.8480	−38.1040	0.0624	0.1648	4.2843	0.2467

for the stretching modes can be qualitatively understood from the variation in the general stability of the molecule. The dianionic clusters with even *n* have higher stability than those with odd *n*, and there is bond strengthening in the structures of the former. The σ mode with the highest frequency consists mostly of the stretching motions of the bonds, this alternating pattern of σ frequency is consistent with the stability of the clusters with even *n*.

3.5. Energy differences

Listed in Table 3 are the electronic states, total energies, energy difference (ΔE_n), electron detachment energy (EDE), second electron detachment energy (SEDE), atomization energy (ΔE_a), and incremental binding energy (ΔE^I) of the "ground-state" C_nS^{2-} ($n = 6$–18) clusters. In the case of triplet state C_nS^{2-} ($n = 6$–16) isomers, spin contamination $\langle S^2 \rangle$ value (before annihilation of the contaminants) is between 2.06 and 2.16, and such small deviation should not have severe effect on our results.

To evaluate the relative stability of the clusters of different sizes, the energy difference $\Delta E_n = E(C_nS^{2-}) - E(C_{n-1}S^{2-})$, which is defined as the difference between the total energies of the adjacent clusters, was calculated. Displayed in Fig. 6 is the variation of energy difference (ΔE_n) of the "ground-state" C_nS^{2-} ($n = 6$–18) clusters versus the number of carbon atoms, i.e., ΔE_n is displayed as a function of *n*. According to the characteristic odd/even alteration, the clusters with even *n* are with ΔE_n lower than those of the adjacent clusters with odd *n*. The observation reiterates that the clusters with even *n* are more stable than those with odd *n*.

3.6. Electron detachment energy and second electron detachment energy

The amount of energy involved in the removal of an electron from a dianion, i.e., the electron detachment energy (EDE, vertical) can be obtained by computing the difference of the total energy of the anionic clusters at optimized dianion geometry and that of optimized dianionic clusters (i.e., $E_{\text{anion}} - E_{\text{optimized dianion}}$). When an EDE of higher value has to be applied for the removal of an electron from a dianion, the dianion is more stable with respect to electron autodetachment. Second electron detachment energy (SEDE, vertical) is computed as the energy difference between the neutral clusters and that of anionic clusters at optimized dianion geometry (i.e., $E_{\text{neutral}} - E_{\text{anion}}$). A higher SEDE would imply that more energy is released when an electron is added to the neutral molecule, and the generation of the respective anion is more readily done. Generally speaking, a corresponding anionic cluster larger in second electron detachment energy is more stable.

Fig. 7 depicts the EDE and SEDE values of the "ground-state" C_nS^{2-} ($n = 6$–18) dianions and the corresponding anions, respectively, versus the number of carbon atoms. The EDE curve of the dianions exhibits odd/even patterns: the EDE of C_nS^{2-} with even *n* is larger than the adjacent C_nS^{2-} of odd *n*, and the level of the EDE value increases with a rise in *n*, indicating that the fragments of C_nS^{2-} with even *n* are more stable than those generated in the decomposition of the adjacent odd-*n* C_nS^{2-} dianions. The SEDE curve is also obvious in odd/even alternation: SEDE of even-*n* clusters are noticeably higher than those of odd-*n* ones. The anions resulted in the fragmentation of

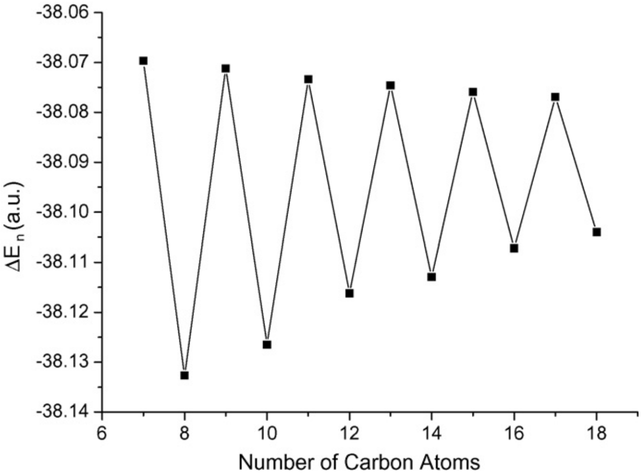

Fig. 6. Energy difference ΔE_n (a.u.) of the "ground-state" C_nS^{2-} ($n = 6$–18) clusters vs. the number of carbon atoms.

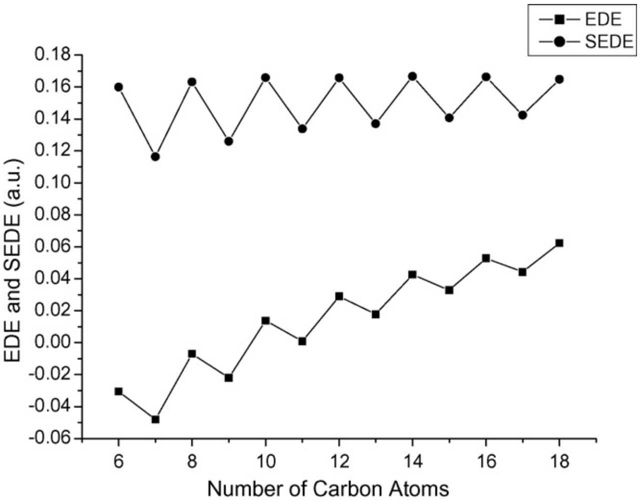

Fig. 7. EDE (a.u.) and SEDE (a.u.) of the “ground-state” C_nS^{2-} ($n = 6$–18) dianions and the corresponding anions, respectively (as shown in Table 3), vs. the number of carbon atoms.

even-n dianions are hence more stable than those generated in the decomposition of odd-n dianions. The overall results of electron detachment with due consideration to the EDE and SEDE values again suggest that the even-n C_nS^{2-} dianions are more stable than the odd-n ones.

For the strong force of Coulomb repulsion of small linear dianions, the determination of electronic stability of dianion is rather delicate. The value of vertical EDE varies with the adopted calculation level. This indefinite prediction concerning the stability with respect to vertical electron detachment was also noticed and discussed by Dreuw and Cederbaum in their study of $BeC_4{}^{2-}$ [29]. According to Table 3, four EDE values are negative (for $n = 6$–9), it suggests that the anions are more stable than the dianions. The electronic stability of dianion for the series with $n = 6$–9 may oscillate between the positive and negative EDE values, depending on the calculation level. In this paper, we focus on the common qualitative trends of odd/even parity alternation rather than the details of electron stability of specific dianions, the EDE deviations caused by the DFT calculation should not have any significant effect on the investigation, and other calculations of higher levels (for example CCSD) cannot afford to achieve such a goal for larger clusters of this kind.

3.7. Incremental binding energies

The incremental binding energy (ΔE^{I}), which is the atomization energy difference (ΔE_a) of adjacent clusters, can also reflect the relative stability of the dianionic clusters [40]. It is expressed as

$$\Delta E^{\mathrm{I}} = \Delta E_{\mathrm{a}}(C_nS^{2-}) - \Delta E_{\mathrm{a}}(C_{n-1}S^{2-});$$

where ΔE_{a} is defined as the energy difference between a molecule and its component atoms:

$$\Delta E_{\mathrm{a}} = nE(\mathrm{C}) + E(\mathrm{S}) - E(C_nS^{2-}).$$

Fig. 8 depicts the incremental binding energies ΔE^{I} (a.u.) of the “ground-state” C_nS^{2-} ($n = 6$–18) clusters versus the number of carbon atoms. As showed in Fig. 8, the values of ΔE^{I} vary according to a pattern of odd/even alternation: when n is even, the ΔE^{I} value is large; when n is odd, the ΔE^{I} is small. Because a larger ΔE^{I} value implies a more stable C_nS^{2-} structure, one can deduce that a C_nS^{2-} cluster with even n is more stable than one with odd n. Such odd/even alternation of electron detachment (EDE and SEDE) and incremental binding energy is in consistency with the experimental observation of Franzreb and Williams [26]. It can be explained by a combined consideration of the overall behaviors of electron detachment (EDE and SEDE) and the incremental binding energies of the dianionic clusters. Since the electron detachment energies and the incremental binding energies of the dianionic clusters are obviously low when n is odd, compared to the even-n clusters, the odd-n ones are less stable and more susceptible to fragmentation.

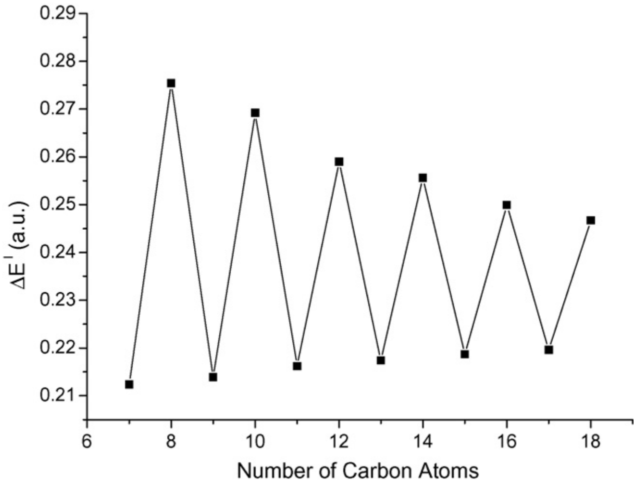

Fig. 8. Incremental binding energies ΔE^{I} (a.u.) of the “ground-state” C_nS^{2-} ($n = 6$–18) clusters (as shown in Table 3) vs. the number of carbon atoms.

4. Conclusions

The “ground-state” structures of C_nS^{2-} ($n = 6$–18) are linear with the sulfur atom located at one end of the C_n chain. When the number of carbon atoms is even, the bond lengths and bond orders suggest a polyacetylene-like structure, whereas when the number of carbon atoms is odd, the data suggest a polyacetylene-like structure with cumulenic-like arrangement close to the chain center. The dianionic clusters with even n are more stable than those with odd n. The regularity of odd/even alternation are illustrated according to the properties of bonding character, atomic charge, electronic configuration, the highest vibrational frequency, energy difference, electron detachment energy, and incremental binding energy. The results of calculation are in agreement with the relative intensity of the C_nS^{2-} ($n = 6$–18) species observed in experimental studies.

Acknowledgments

The authors thank the National Science Foundation (Grants 20473061, 20423002 and 20533020) for financial supports.

Appendix A. Supplementary data

Supplementary data associated with this article can be found, in the online version, at doi:10.1016/j.ijms.2006.11.005.

References

[1] W. Weltner Jr., R.J. Van Zee, Chem. Rev. 89 (1989) 1713.
[2] G. von Helden, N.G. Gotts, M.T. Bowers, Nature 363 (1993) 6424.
[3] J. Cernicharo, M. Guelin, H. Hein, C. Kahane, Astron. Astrophys. 181 (1987) L9.
[4] S. Yamamoto, S. Saito, K. Kawaguchi, N. Kaifu, H. Suzuki, Astrophys. J. 317 (1987) L119.
[5] M.B. Bell, L.W. Avery, P.A. Feldman, Astrophys. J. 417 (1993) L37.
[6] D. Consalvo, A. Mele, D. Stranges, A. Giardini-Guidoni, R. Teghil, Int. J. Mass Spectrom. Ion Processes 91 (1989) 319.
[7] M. Leleyter, P. Joyes, Surf. Sci. 156 (1985) 800.
[8] S. Becker, H.-J. Dietze, Int. J. Mass Spectrom. Ion Processes 82 (1988) 287.
[9] R.B. Huang, C.R. Wang, Z.Y. Liu, L.S. Zheng, F. Qi, L.S. Sheng, S.Q. Yu, Y.W. Zhang, Z. Phys. D 33 (1995) 49.
[10] Z.Y. Liu, R.B. Huang, L.S. Zheng, Z. Phys. D 38 (1996) 171.
[11] A. Zaidi, S. Lahmar, Z. Ben Lakhdar, P. Rosmus, M. Hochlaf, Theor. Chem. Acc. 114 (2005) 341.
[12] H.Y. Wang, J. Szczepanski, P. Brucat, M. Vala, Int. J. Quantum Chem. 102 (2005) 795.
[13] H.Y. Wang, J. Szczepanski, A. Cooke, P. Brucat, M. Vala, Int. J. Quantum Chem. 102 (2005) 806.
[14] I. Pérez-Juste, A.M. Graña, L. Carballeira, R.A. Mosquera, J. Chem. Phys. 121 (2004) 10447.
[15] Z.C. Tang, J.J. BelBruno, Int. J. Mass Spectrom. 208 (2001) 7.
[16] S. Lee, Chem. Phys. Lett. 268 (1997) 69.
[17] K.H. Kim, B. Lee, S. Lee, Chem. Phys. Lett. 297 (1998) 65.
[18] G. Pascoli, H. Lavendy, Int. J. Mass Spectrom. 181 (1998) 11.
[19] G. Pascoli, H. Lavendy, Int. J. Mass Spectrom. 181 (1998) 135.
[20] J.R. Flores, I.P. Juste, L. Carballeira, C. Estevez, F. Gomez, Chem. Phys. Lett. 343 (2001) 105.
[21] A. Dreuw, L.S. Cederbaum, Chem. Rev. 102 (2002) 181.
[22] S.N. Schauer, P. Williams, R.N. Compton, Phys. Rev. Lett. 65 (1990) 625.
[23] J. Klein, R. Middleton, Nucl. Instrum. Methods Phys. Res. B 159 (1999) 8.
[24] H. Gnaser, Phys. Rev. A 60 (1999) R2645.
[25] H. Gnaser, A. Dreuw, L.S. Cederbaum, J. Chem. Phys. 117 (2002) 7002.
[26] K. Franzreb, P. Williams, J. Chem. Phys. 123 (2005) 224312.
[27] A. Dreuw, T. Sommerfeld, L.S. Cederbaum, J. Chem. Phys. 109 (1998) 2727.
[28] A. Dreuw, T. Sommerfeld, L.S. Cederbaum, Angew. Chem. Int. Ed. Engl. 36 (1997) 1889.
[29] A. Dreuw, L.S. Cederbaum, J. Chem. Phys. 112 (2000) 7400.
[30] Q.C. Shi, S. Kais, J. Am. Chem. Soc. 124 (2002) 11723.
[31] C. Trindle, A. Yumak, J. Chem. Theory Comput. 1 (2005) 1038.
[32] M.D. Chen, X.B. Li, J. Yang, Q.E. Zhang, C.T. Au, J. Phys. Chem. A 110 (2006) 4502.
[33] Hypercube Inc., Hyerchem Reference Manual, Waterloo, Ont., Canada, 1996.
[34] M. James, C. Crabbe, J.R. Appleyard, C.R. Lay, Desktop Molecular Modeller, Oxford University Press, Walton Street, Oxford, Great Britain, 1994.
[35] M.J. Frisch, G.W. Trucks, H.B. Schlegel, G.E. Scuseria, M.A. Robb, J.R. Cheeseman, J.A. Montgomery Jr., T. Vreven, K.N. Kudin, J.C. Burant, J.M. Millam, S.S. Iyengar, J. Tomasi, V. Barone, B. Mennucci, M. Cossi, G. Scalmani, N. Rega, G.A. Petersson, H. Nakatsuji, M. Hada, M. Ehara, K. Toyota, R. Fukuda, J. Hasegawa, M. Ishida, T. Nakajima, Y. Honda, O. Kitao, H. Nakai, M. Klene, X. Li, J.E. Knox, H.P. Hratchian, J.B. Cross, C. Adamo, J. Jaramillo, R. Gomperts, R.E. Stratmann, O. Yazyev, A.J. Austin, R. Cammi, C. Pomelli, J.W. Ochterski, P.Y. Ayala, K. Morokuma, G.A. Voth, P. Salvador, J.J. Dannenberg, V.G. Zakrzewski, S. Dapprich, A.D. Daniels, M.C. Strain, O. Farkas, D.K. Malick, A.D. Rabuck, K. Raghavachari, J.B. Foresman, J.V. Ortiz, Q. Cui, A.G. Baboul, S. Clifford, J. Cioslowski, B.B. Stefanov, G. Liu, A. Liashenko, P. Piskorz, I. Komaromi, R.L. Martin, D.J. Fox, T. Keith, M.A. Al-Laham, C.Y. Peng, A. Nanayakkara, M. Challacombe, P.M.W. Gill, B. Johnson, W. Chen, M.W. Wong, C. Gonzalez, J.A. Pople, Gaussian 03 (Revision B.05), Gaussian, Inc., Pittsburgh, PA, 2003.
[36] A.D. Becke, J. Chem. Phys. 98 (1993) 5648.
[37] C. Lee, W. Yang, R.G. Parr, Phys. Rev. B 37 (1988) 785.
[38] J.B. Foresman, Æ. Frisch, Exploring Chemistry with Electronic Structure Methods, Gaussian Inc., Pittsburgh, PA, 1996.
[39] D.C. Parent, S.L. Anderson, Chem. Rev. 92 (1992) 1541.
[40] G. Pascoli, H. Lavendy, Int. J. Mass Spectrom. Ion Processes 173 (1998) 41.